

# Single Amino Acid Substitutions in Flexible Loops Can Induce Large Compressibility Changes in Dihydrofolate Reductase<sup>1</sup>

Kunihiko Gekko,<sup>2</sup> Tadashi Kamiyama, Eiji Ohmae, and Katsuo Katayanagi

Department of Mathematical and Life Sciences, Graduate School of Science, Hiroshima University, Higashi-Hiroshima 739-8526

Received February 14, 2000; accepted April 10, 2000

To address the effects of single amino acid substitutions on the flexibility of *Escherichia coli* dihydrofolate reductase (DHFR), the partial specific volume ( $\bar{v}^\circ$ ) and adiabatic compressibility ( $\beta_s^\circ$ ) were determined for a series of mutants with amino acid replacements at Gly67 (7 mutants), Gly121 (6 mutants), and Ala145 (5 mutants) located in three flexible loops, by means of precise sound velocity and density measurements at 15°C. These mutations induced large changes in  $\bar{v}^\circ$  (0.710–0.733 cm<sup>3</sup>·g<sup>-1</sup>) and  $\beta_s^\circ$  ( $-1.8 \times 10^{-6}$ – $5.5 \times 10^{-6}$  bar<sup>-1</sup>) from the corresponding values for the wild-type enzyme ( $\bar{v}^\circ = 0.723$  cm<sup>3</sup>·g<sup>-1</sup>,  $\beta_s^\circ = 1.7 \times 10^{-6}$  bar<sup>-1</sup>), probably due to modifications of internal cavities. The  $\beta_s^\circ$  value increased with increasing  $\bar{v}^\circ$ , but showed a decreasing tendency with the volume of the amino acid introduced. There was no significant correlation between  $\beta_s^\circ$  and the overall stability of the mutants determined from urea denaturation experiments. However, a mutant with a large  $\beta_s^\circ$  value showed high enzyme activity mainly due to an enhanced catalytic reaction rate ( $k_{\text{cat}}$ ) and in part due to increased affinity for the substrate ( $K_m$ ), despite the fact that the mutation sites are far from the catalytic site. These results demonstrate that the flexibility of the DHFR molecule is dramatically influenced by a single amino acid substitution in one of these loops and that the flexible loops of this protein play important roles in determining the enzyme function.

**Key words:** amino acid substitution, compressibility, dihydrofolate reductase, flexible loops, structural flexibility.

How does a single amino acid substitution in a protein affect the flexibility or fluctuation of its structure? This is a basic problem in understanding the structure–function relationship of enzymes, but information in this area is limited despite many mutation studies (1–3). Among various experimental techniques related to the magnitude and time scale of protein structure fluctuation (4–7), compressibility is a novel measure of structural flexibility in solution since it is directly linked to volume fluctuation (8). Although volume fluctuation is a thermodynamic quantity involving the effects of internal cavities and surface hydration, the partial specific adiabatic compressibility,  $\beta_s^\circ$ , is known to reflect sensitively the structural characteristics of native proteins (9–11), the conformational changes caused by denaturation (12–14), and the effect of ligand binding (15–17). So far, however, because of technical difficulties, only a preliminary study has been reported concerning the compressibility of mutants of two *Escherichia coli* proteins, dihydrofolate reductase and aspartate aminotransferase (18).

Dihydrofolate reductase (DHFR) from *E. coli* is an excel-

lent system for studying the structure–flexibility–function relationships of enzymes. It is a monomeric protein of 159 amino acids with no disulfide bonds and catalyzes the NADPH-linked reduction of dihydrofolate (DHF) to tetrahydrofolate (THF). The X-ray crystal structure of DHFR has been determined for the apoenzyme (19) and for the binary and ternary complexes with many ligands (20). As shown in Fig. 1, DHFR has several flexible loops with large B-factors, namely residues 9–24, 64–72, 117–131, and 142–149 (20). The B-factors of these loops are remarkably affected by the binding of the inhibitor methotrexate (MTX), suggesting the participation of the loops in the enzymatic function. We found that site-directed mutagenesis at Gly67, Gly121, and Ala145 in the three loops exerts a significant influence on the stability and function of the enzyme, despite these positions being far removed from the catalytic residue Asp27 (21–24). Interestingly, double mutants at Gly67 and Gly121, whose  $\alpha$ -carbons are mutually separated by 27.7 Å, show nonadditive effects on the stability and function (25). These results suggest that these mutations alter the flexibility of the entire molecule. Therefore, a systematic compressibility study of these mutants is expected to shed light on the question of how a single amino acid substitution is linked to the flexibility of this enzyme.

From this viewpoint, we determined the partial specific volume and adiabatic compressibility of DHFR for a series of mutants at Gly67 (7 mutants), Gly121 (6 mutants), and Ala145 (5 mutants) in three different flexible loops, by means of precise sound velocity and density measurements.

<sup>1</sup> This work was supported by a Grant-in-Aid (No. 10480159) for Scientific Research from the Ministry of Education, Science, Sports and Culture of Japan, and in part by the Sasagawa Scientific Research Grant from The Japan Science Society

<sup>2</sup> To whom correspondence should be addressed. Fax: +81-824-24-7387, E-mail: gekko@sci.hiroshima-u.ac.jp  
Abbreviations: DHF, dihydrofolate; DHFR, dihydrofolate reductase; MTX, methotrexate; THF, tetrahydrofolate.

Based on the results, the relationship between the flexibility and the structure, stability and function in the enzyme will be discussed in terms of the internal cavity and surface hydration.

#### MATERIALS AND METHODS

**Materials**—All mutant DHFR genes were prepared with plasmids pTP64-1 (5.3 kb) and pTZwt1-3 (3.7 kb), which produced 840- and 1,400-fold overexpression of the wild-type DHFR protein, respectively (26, 27). The oligonucleotides used for site-directed mutagenesis and the detailed mutant construction were described in previous papers (22–24). The wild-type and all mutant DHFRs obtained from *E. coli* strain HB101 were purified on a methotrexate-agarose affinity column. The enzymes were fully dialyzed against 10 mM phosphate buffer (pH 7.0) containing 0.1 mM EDTA and 0.1 mM dithiothreitol at 4°C. The dialyzed solution thus obtained was centrifuged at 14,000 rpm for 20 min to remove the aggregates. Five or six sample solutions of different enzyme concentrations (0.2–0.8%) were prepared by diluting the dialyzed stock solution with the dialysate.

The concentrations of all DHFRs were determined by absorption measurements on a Shimadzu spectrophotometer UV-250, after sound velocity and density measurements. A molar extinction coefficient of 31,100 M<sup>-1</sup>·cm<sup>-1</sup> at 280 nm was used for the wild-type DHFR (28). For the mutants, this coefficient was corrected using the molecular weights and chromophores of the amino acids introduced.

**Sound Velocity and Density Measurements**—The partial specific volume,  $\bar{v}^\circ$ , and partial specific adiabatic compressibility,  $\beta_s^\circ$ , of DHFRs were determined by sound velocity and density measurements at 15°C. The sound velocity in

protein solutions was measured by means of a “sing-around pulse method” at 5.9 MHz with an accuracy of 1 cm·s<sup>-1</sup>. The density was measured with a precision density meter, DMA-02C (Anton Paar, Gratz), with an accuracy of 1 × 10<sup>-6</sup> g·cm<sup>-3</sup>. The temperature was controlled to an accuracy of 0.01°C using a thermbath (Neslab RTE-111). The apparatus and experimental procedures were essentially the same as those previously used (10, 12, 17).

The adiabatic compressibilities of the sample solution ( $\beta$ ) and solvent ( $\beta_0$ ) were calculated with the Laplace equation,  $\beta = 1/du^2$ , using the sound velocity ( $u$ ) and density ( $d$ ) data set for the sample solution and solvent ( $u_0$  and  $d_0$ ). The partial specific volume,  $\bar{v}^\circ$ , and adiabatic compressibility of the protein,  $\beta_s^\circ$ , at infinite dilution were calculated using the following equations (9, 10):

$$\bar{v}^\circ = \lim_{c \rightarrow 0} (1 - V_0)/c \quad (1)$$

$$\beta_s^\circ = - (1/\bar{v}^\circ) (\delta\bar{v}^\circ / \delta P) = (\beta/\bar{v}^\circ) \lim_{c \rightarrow 0} (\beta/\beta_0 - V_0)/c \quad (2)$$

$$V_0 = (d - c)/d_0 \quad (3)$$

where  $P$  is the pressure,  $V_0$  the apparent volume fraction of the solvent in solution, and  $c$  the concentration of the protein in grams per milliliter of solution.

#### RESULTS AND DISCUSSION

The density,  $d$ , and sound velocity,  $u$ , of all DHFR solutions increased in proportion to the protein concentration. The density and sound velocity increments per unit protein concentration,  $\delta d/\delta c$  and  $\delta u/\delta c$ , are listed in Table I. The variations of  $\delta d/\delta c$  ( $\pm 4\%$ ) and  $\delta u/\delta c$  ( $\pm 12\%$ ) by mutation are beyond the limits of possible experimental error caused by the concentration determination of each mutant, indicating the characteristic changes in the partial specific volume and adiabatic compressibility by mutation.

Figure 2 shows typical plots of the  $(1 - V_0)/c$  and  $(\beta/\beta_0 - V_0)/c$  against

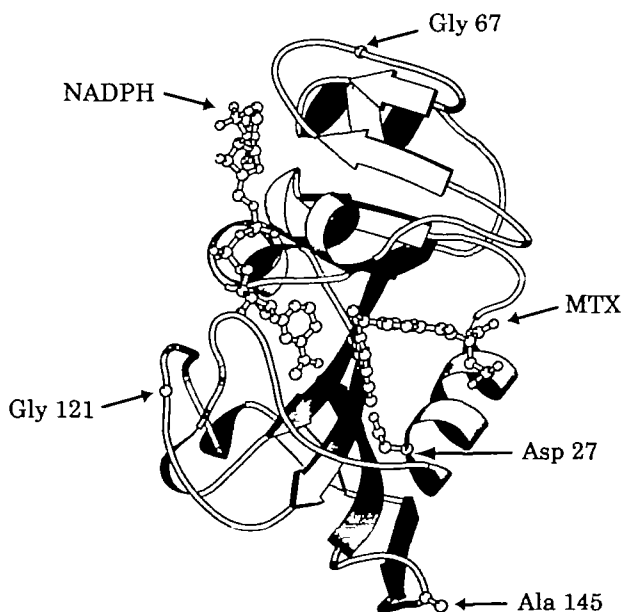


Fig. 1. The structure of a DHFR-MTX-NADPH ternary complex (PDB-ID: 1rx3) taken from Sawaya and Kraut (20). Positions Gly67, Gly121, Ala145, and Asp27 (a catalytic site residue) are indicated by arrows. The side chains of Ala145 and Asp27 are shown by ball-and-stick models. This figure was produced using the graphics program Molscript (38).

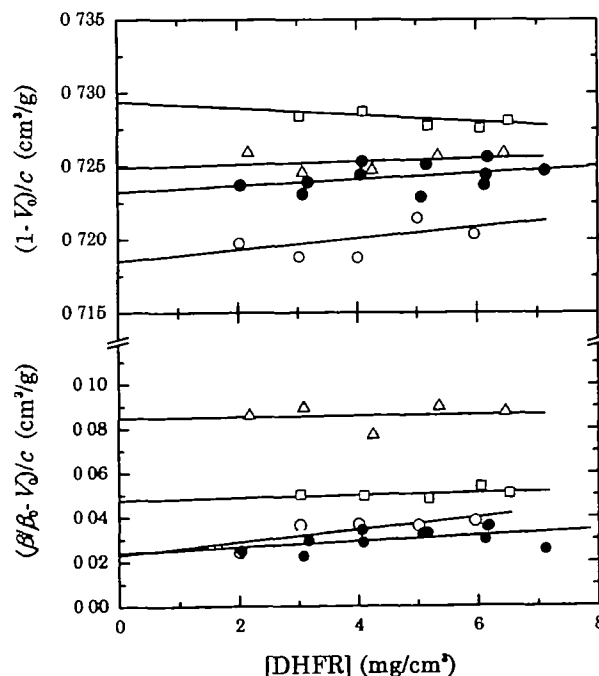


Fig. 2. Typical plots of  $(1 - V_0)/c$  and  $(\beta/\beta_0 - V_0)/c$  against DHFR concentration. Solid lines represent the least-squares linear regression ●, wild-type, ○, G67T; △, G121C; □, A145T

$V_p/c$  values against the concentration of the wild-type and some mutant DHFRs. No significant concentration dependence of the two parameters was observed in the protein concentration range investigated, suggesting a negligibly small contribution of aggregation or self-association. The  $\bar{v}^\circ$  and  $\bar{\beta}_s^\circ$  values at infinite dilution were calculated by least-squares linear regression and the results of the calculation are listed in the fourth and fifth columns of Table I. Interestingly, a single amino acid substitution brought about large variations in  $\bar{v}^\circ$  ( $0.710$ – $0.733 \text{ cm}^3\cdot\text{g}^{-1}$ ) and  $\bar{\beta}_s^\circ$  ( $-1.8 \times 10^{-6}$ – $5.5 \times 10^{-6} \text{ bar}^{-1}$ ) from the corresponding values for the wild-type enzyme ( $\bar{v}^\circ = 0.723 \text{ cm}^3 \text{ g}^{-1}$  and  $\bar{\beta}_s^\circ = 1.7 \times 10^{-6} \text{ bar}^{-1}$ ). The effects of mutation seem to be dependent on the mutation sites: position 121 has the largest mutation effects compared with positions 67 and 145. The  $\bar{v}^\circ$  and  $\bar{\beta}_s^\circ$  values for the wild-type and some mutant DHFRs at position 121 differ considerably from those reported in a previous paper (18). This discrepancy is ascribed to insufficient centrifugation (4,000 rpm for 15 min) of the sample solutions. Thus the  $\bar{v}^\circ$  and  $\bar{\beta}_s^\circ$  data previously reported for the wild-type and some mutant DHFRs at position 121 should be corrected to the values listed in Table I, which were obtained by carefully eliminating aggregates from the sample solutions.

The variation of  $\bar{\beta}_s^\circ$  by mutation indicates that small structural alterations around the mutation sites significantly influence the flexibility or overall dynamics of this enzyme. This is consistent with the findings that these mutations bring about noticeable changes in the stability and function of this enzyme even though the mutation sites are far from the catalytic residue Asp27 (21–24). A matter of concern is how a single amino acid substitution induces the overall structure change, leading to the alterations in flexibility, stability, and function. This problem will be dis-

cussed below through the correlation between  $\bar{\beta}_s^\circ$  and some physical quantities related to the structure, stability, and function of the mutants.

**Compressibility–Structure Relationship**—The partial specific volume of a protein in water is expressed as the sum of three contributions (29): (i) the constitutive volume estimated as the sum of the constitutive atomic volumes ( $v_c$ ); (ii) the cavity in the molecule due to imperfect atomic packing ( $v_{\text{cav}}$ ); (iii) the volume change due to hydration ( $\Delta v_{\text{sol}}$ ):

$$\bar{v}^\circ = v_c + v_{\text{cav}} + \Delta v_{\text{sol}} \quad (4)$$

where  $\Delta v_{\text{sol}}$  is ascribed to three types of hydration, electrostriction around the ionic groups, hydrogen-bonded hydration around the polar groups, and hydrophobic hydration around the nonpolar groups. Each type of hydration produces a negative volume change, so  $\Delta v_{\text{sol}}$  is ordinarily nega-

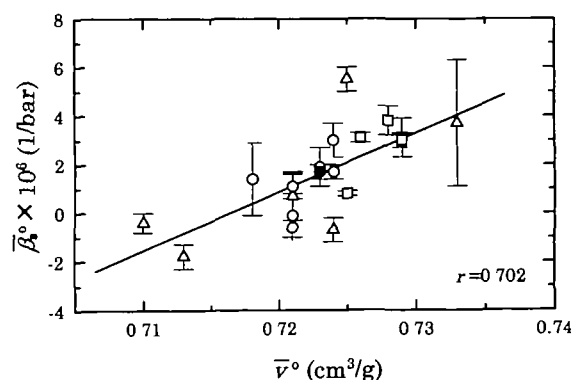


Fig 3 Plots of  $\bar{\beta}_s^\circ$  against  $\bar{v}^\circ$  of DHFRs at 15°C. ●, wild-type, ○, G67 mutants, △, G121 mutants, □, Ala145 mutants. Solid line represents the least-squares linear regression with the correlation coefficient,  $r$

TABLE I Partial specific volume ( $\bar{v}^\circ$ ), adiabatic compressibility ( $\bar{\beta}_s^\circ$ ), thermal stability, and enzyme activity of DHFR mutants.\*

DHFRs	$\delta d/\delta c \times 10$	$\delta u/\delta c$ ( $\text{m}\cdot\text{cm}^3/\text{g}\cdot\text{s}$ )	$\bar{v}^\circ$ ( $\text{cm}^3/\text{g}$ )	$\bar{\beta}_s^\circ \times 10^6$ (1/bar)	$\Delta G^\circ$ (kcal/mol)	$C_m$ (M)	$m$ (kcal/mol M)	$K_m$ ( $\mu\text{M}$ )	$k_{\text{cat}}$ (1/s)	$k_{\text{cat}}/K_m$ ( $1/\mu\text{M}\cdot\text{s}$ )
wild	2.764±0.007	307.7±3.1	0.723±0.001	1.7±0.3	6.08	3.11	-1.96	1.3	24.6	18.9
G67S	2.740±0.006	311.4±5.3	0.723±0.003	1.9±0.8	6.15	2.82	-2.18	1.4	26.4	18.9
G67A	2.796±0.008	323.5±4.0	0.721±0.002	-0.1±0.9	6.60	2.82	-2.34	1.1	20.0	18.2
G67C	2.760±0.026	310.6±1.1	0.724±0.001	1.7±0.3	5.72	2.79	-2.05	1.2	24.6	20.5
G67D	2.685±0.009	309.2±3.5	0.724±0.003	3.0±0.7	5.94	2.62	-2.27	1.2	20.6	17.2
G67T	2.792±0.005	295.3±2.3	0.718±0.002	1.4±1.5	5.87	2.62	-2.24	1.8	26.6	14.8
G67V	2.752±0.009	318.7±2.0	0.721±0.003	1.1±0.5	5.14	2.89	-1.78	1.3	19.1	14.7
G67L	2.822±0.009	321.5±9.4	0.721±0.003	-0.6±1.4	5.64	2.83	-1.99	1.1	22.6	20.5
G121S	2.780±0.006	308.5±4.5	0.721±0.002	0.7±1.0	6.09	3.03	-2.01	1.8	5.2	2.9
G121A	2.901±0.009	313.5±7.8	0.710±0.003	-0.4±0.4	6.58	2.86	-2.30	2.7	8.5	3.1
G121C	2.741±0.002	271.0±3.0	0.725±0.001	5.5±0.5	6.17	2.86	-2.16	1.5	8.4	5.6
G121V	2.653±0.006	283.5±5.6	0.733±0.003	3.7±2.6	5.09	2.65	-1.92	1.4	0.94	0.67
G121H	2.786±0.005	345.3±4.6	0.713±0.002	-1.8±0.5	5.97	2.64	-2.26	2.2	4.8	2.2
G121Y	2.819±0.013	344.5±3.0	0.724±0.001	-0.7±0.6	5.88	2.72	-2.16	2.5	4.4	1.8
A145G	2.727±0.003	294.1±1.2	0.726±0.001	3.1±0.2	7.38	3.05	-2.42	1.2	21.2	17.6
A145S	2.698±0.004	303.7±2.4	0.729±0.002	3.1±0.8	7.28	3.05	-2.38	0.8	19.3	24.1
A145T	2.714±0.002	306.4±3.5	0.729±0.001	3.0±0.3	9.13	3.10	-2.95	1.6	20.0	12.5
A145H	2.730±0.006	303.8±3.4	0.728±0.001	3.8±0.6	7.25	2.97	-2.44	0.8	18.8	26.9
A145R	2.744±0.001	322.0±2.0	0.725±0.002	0.8±0.1	8.05	3.26	-2.48	1.4	19.9	14.2

\* $\delta d/\delta c$  and  $\delta u/\delta c$  represent the density and sound velocity increments per unit protein concentration, respectively.  $\Delta G^\circ$ ,  $C_m$ , and  $m$  are the free energy change of urea denaturation, the urea concentration at the mid point of the transition, and the parameter reflecting the cooperativity of the unfolding transition, respectively.  $K_m$  and  $k_{\text{cat}}$  represent the Michaelis constant and the rate constant of catalysis, respectively. These parameters for the stability and enzyme activity were taken from previous papers (22–24).

tive. Since the constitutive atomic volume may be assumed to be incompressible, the partial specific adiabatic compressibility of a protein ( $\bar{\beta}_s^\circ$ ) is mainly determined by the internal cavity and surface hydration as follows (9, 10):

$$\bar{\beta}_s^\circ = -(1/\bar{v}^\circ)(\delta\bar{v}^\circ/\delta P) = (1/\bar{v}^\circ)[(\delta v_{\text{cav}}/\delta P) + (\delta\Delta v_{\text{surf}}/\delta P)] \quad (5)$$

The former contributes positively and the latter negatively to  $\bar{\beta}_s^\circ$ , so  $\bar{\beta}_s^\circ$  can take a positive or negative value depending on the magnitude of each term.

Figure 3 shows plots of  $\bar{\beta}_s^\circ$  against  $\bar{v}^\circ$  for the wild-type and mutant DHFRs. Evidently, the  $\bar{\beta}_s^\circ$  value increases with increasing  $\bar{v}^\circ$ , as found statistically for other protein systems (10). This is evidence that the cavity contributes positively and the hydration negatively to both parameters,  $\bar{v}^\circ$  and  $\bar{\beta}_s^\circ$ , because the change of  $v_c$  by mutation is at most  $0.001 \text{ cm}^3 \cdot \text{g}^{-1}$ , which is within the experimental error of  $\bar{v}^\circ$ . As shown in Table II, in fact, there is no correlation between  $\bar{v}^\circ$  and the volume of the amino acid residue introduced ( $V$ ) at any mutation site except position 67, at which a slightly negative correlation seems to exist.

On the other hand, there is a slightly negative correlation between  $\bar{\beta}_s^\circ$  and  $V$  at all mutation sites. Plots of  $\bar{\beta}_s^\circ$  against the volume change of amino acids ( $\Delta V$ ) due to mutation (Fig. 4) suggest more clearly that the structural flexibility is depressed by introducing a bulky amino acid side chain in these loops. This would be possible if the mutation exerts a dominant effect on the internal cavity or atomic packing of the protein molecule compared with surface hydration. A computer simulation predicts that Gly67 and Gly121 cannot be replaced by any other amino acid without accompanying movements of the backbone polypeptide chain due to changes in the torsion angles  $\chi_1$  and  $\chi_2$  of the side chains being directed toward the inside of the protein molecule (S. Segawa, personal communication). This implies that mutations at these positions may influence not only the local atomic packing around the side chains of the replaced amino acid residues, but also the internal cavity throughout the protein molecule *via* the long-range interaction effects.

In a previous paper (10), we analyzed statistically the contributions of 20 different amino acid residues on  $\bar{\beta}_s^\circ$  of 23 globular proteins and found that four amino acid residues (Leu, Glu, Phe, and His) greatly increase  $\bar{\beta}_s^\circ$  and four others (Asn, Gly, Ser, and Thr) decrease it. Such a statistical rule cannot necessarily fit the present case for DHFR: the mutations Gly  $\rightarrow$  Leu at position 67 and Gly  $\rightarrow$  His at position 121 decreased  $\bar{\beta}_s^\circ$ , the opposite of the expectation.

Much more precise analysis based on the X-ray crystal structure is necessary to predict mutation effects on  $\bar{\beta}_s^\circ$ .

Recently, we carried out X-ray crystallographic analyses of some DHFR mutants at positions 67 and 121, and found that the B-factors of the main chain atoms and the cavities at positions far from the mutation sites are influenced by mutation without any significant change in the accessible surface area (K. Katayama *et al.*, to be published). Interestingly, the total cavity volume of the mutants decreased with decreasing  $\bar{\beta}_s^\circ$ . Therefore, we could ascribe the main origin of the mutation-induced  $\bar{\beta}_s^\circ$  changes to modification of internal cavities: overcrowding of a bulky amino acid would not contribute to expanding the flexible loops, but rather to packing the internal atoms more densely. It is very possible that only a small modification of cavities causes a large compressibility change because the apparent compressibility of a cavity,  $\beta_{\text{cav}}$  is very large, *e.g.*,  $(430\text{--}530) \times 10^{-6} \text{ bar}^{-1}$  for bovine serum albumin at  $25^\circ\text{C}$  (9). Assuming the negligibly small contribution of hydration, we might predict a smaller  $\beta_{\text{cav}}$  value,  $(160\text{--}200) \times 10^{-6} \text{ bar}^{-1}$ , for the cavities of these DHFR mutants at  $15^\circ\text{C}$ , based on the slopes of the  $\bar{v}^\circ\bar{\beta}_s^\circ\text{--}\bar{v}^\circ$  plots (figure not shown). A similar  $\beta_{\text{cav}}$  value,  $(240\text{--}330) \times 10^{-6} \text{ bar}^{-1}$ , was obtained from the dependence of  $\bar{\beta}_s^\circ$  on the total cavity volume calculated from the X-ray crystal structures of the DHFR mutants. These  $\beta_{\text{cav}}$  values are still 5-fold larger than the adiabatic compressibility of free water ( $45 \times 10^{-6} \text{ bar}^{-1}$ ), enough for com-

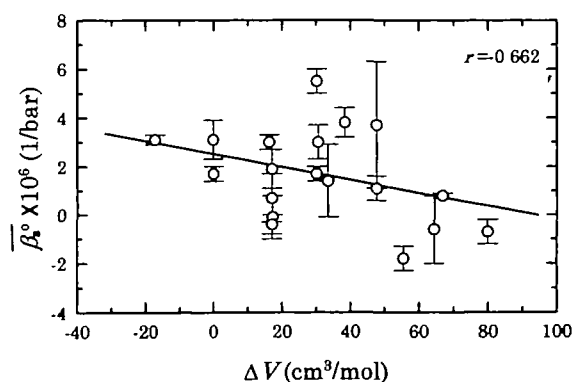


Fig 4 Plots of  $\bar{\beta}_s^\circ$  against  $\Delta V$ , the volume change of amino acid side chains due to mutation of DHFR, at  $15^\circ\text{C}$ . Solid line represents the least-squares linear regression.

TABLE II. Correlation coefficients ( $r$ ) of  $\bar{v}^\circ$  and  $\bar{\beta}_s^\circ$  for the volume of amino acid residues introduced, stability, and enzyme activity of DHFR mutants.

Mutation site <sup>a</sup>	Amino acid <sup>b</sup>	Stability			Function		
		$V$	$\Delta G^\circ$	$C_m$	$K_m$	$k_{\text{cat}}$	$k_{\text{cat}}/K_m$
Correlation for $\bar{v}^\circ$							
G67	(7)	-0.36	-0.10	0.25	-0.59	-0.09	0.58
G121	(6)	0.18	-0.79	-0.08	-0.70	-0.62 <sup>c</sup>	-0.23 <sup>c</sup>
A145	(5)	-0.03	0.60	-0.48	-0.31	-0.81	0.25
Correlation for $\bar{\beta}_s^\circ$							
G67	(7)	-0.44	-0.04	-0.23	0.31	0.23	-0.23
G121	(6)	-0.27	-0.31	0.16	-0.75	0 <sup>c</sup>	0.41 <sup>c</sup>
A145	(5)	-0.44	0.08	-0.94	-0.54	-0.44	0.56

<sup>a</sup>Numbers in parentheses are the number of mutants at each mutation site. <sup>b</sup>Volumes of the amino acid residues ( $V$ ) used: Gly, 34.8, Ala, 52.0; Val, 82.4, Leu, 99.2; Thr, 68.3; Ser, 51.9; Asp, 65.4; His, 90.3; Tyr, 114.7; Arg, 118.8; Cys, 65.0 ml/mol (39) <sup>c</sup>Data for the wild-type DHFR were eliminated for regression.

pression of the protein molecule. At present, we have no X-ray structural data for mutants at position 145, so it is unknown whether similar overcrowding effects exist at this position at which the side chain of alanine (wild-type) is exposed to the solvent. However, it is probable that mutations at this position also influence the internal cavity through modified flexibility of the loop or penetration of amino acid side chains into the protein molecule. A more detailed understanding of the mutation effects in the loop regions requires information on not only the mutation sites but also on the direction of the amino acid side chains introduced.

**Compressibility–Stability Relationship**—The Gibbs free energy change of urea denaturation,  $\Delta G^\circ$ , the urea concentration at the mid point of the transition,  $C_m$ , and the parameter reflecting the cooperativity of the unfolding transition,  $m$ , for the wild-type and mutant DHFRs are listed in Table I (22–24). Evidently, the mutations at the three positions affect the structural stability; in most cases the stability is decreased by mutations at positions 67 and 121 but increased by mutations at position 145. The correlation coefficients of  $\bar{v}^\circ$  and  $\bar{\beta}_s^\circ$  with these thermodynamic parameters were calculated by least-squares linear regression analysis for the data set at each mutation site including those for the wild-type DHFR. The results of the calculations are listed in Table II.

No significant correlation was observed between  $\bar{\beta}_s^\circ$  and  $\Delta G^\circ$ , although there seemed to be a slightly negative correlation at position 121. This is inconsistent with the results of statistical analysis showing that the  $\Delta G^\circ$  per unit mass of protein decreases with increasing  $\bar{\beta}_s^\circ$  (30). Thus the stability of these DHFR mutants cannot be interpreted simply by a general idea that a rigid protein is more stable than a flexible one. It is not unlikely that  $\bar{\beta}_s^\circ$  has no correlation with  $\Delta G^\circ$  because the former refers to the native state only while the latter is the difference in the free energies of a protein in the native and denatured states. A noticeable characteristic observed for the stability of these mutants is that the  $\Delta G^\circ$  value decreases with concomitant increases in the volume and hydrophobicity of the introduced amino acids (22–24). This result has been explained by each of two possible mechanisms: (i) the flexibility of the loops enhanced by overcrowding of the bulky side chains overcomes the stabilizing effect of hydrophobic interaction, leading to destabilization of the native state; and (ii) the denatured state is more strongly stabilized by hydrophobic interactions than the native state (reverse hydrophobic effect), as proposed for mutations at hyper or highly exposed positions (31, 32). At present, there is no direct experimental evidence for either of these mechanisms. However, the first would not be satisfactory in the present case because, as discussed above, the compressibility is decreased oppositely by introducing bulky amino acids into the mutation sites. Thus the hydrophobic effect of the introduced amino acids on the denatured state might overcome the volume effect on the native state, leading to stabilization of the denatured state.

There was also no significant correlation found between  $\bar{\beta}_s^\circ$  and  $m$ , although a slightly positive correlation was found at position 121. This suggests that the cooperativity of unfolding is not directly linked to the flexibility of the protein structure, probably because the parameter  $m$  is proportional to the difference in the solvent-accessible sur-

face areas of a protein in the native and denatured states (33, 34). Therefore, it is difficult to understand the compressibility–stability relationship without considering the mutation effects on the denatured state.

**Compressibility–Function Relationship**—The steady-state kinetic parameters,  $K_m$  and  $k_{cat}$ , for the enzyme reaction of DHFRs are listed in Table I (22–24). The  $K_m$  is only slightly influenced by mutations at the three positions, but  $k_{cat}$  changes significantly, especially by mutation at position 121, resulting in a large modification of the enzyme activity ( $k_{cat}/K_m$ ). This is very interesting because it is unlikely that the mutation sites participate directly in the enzyme reaction: the  $\alpha$ -carbons of Gly67, Gly121, and Ala145 are separated, respectively, by 29.3, 19.0, and 14.4 Å from the catalytic site Asp27, and are at shortest 8.5, 10.6, and 29.2 Å from the NADPH molecule (20). Table II shows the correlation coefficients of  $\bar{v}^\circ$  and  $\bar{\beta}_s^\circ$  with the kinetic parameters at each mutation site. These correlation coefficients are together not so large, but it is noteworthy that  $\bar{\beta}_s^\circ$  correlates negatively with  $K_m$  and positively with  $k_{cat}/K_m$  at positions 121 and 145. As shown in Fig. 5a, plots of  $K_m$  against  $\bar{\beta}_s^\circ$  indicate more conclusively the negative correlation ( $r = -0.632$ ) if the data points for all mutants except three, G67T, G67L, and G121V, which have large experimental errors of  $\bar{\beta}_s^\circ$  ( $> \pm 1 \times 10^{-6}$  bar $^{-1}$ ), are used. This correlation suggests that the structural flexibility contributes favorably to this enzyme binding the substrate, DHF, probably by accelerating the on-rate rather than the off-rate of the substrate binding reaction. Furthermore, as shown in Fig. 5b, a positive correlation ( $r = 0.552$ ) was found between  $\log(k_{cat}/K_m)$  and  $\bar{\beta}_s^\circ$  for all the mutants except the above three, mainly due to the similar positive correlation between  $k_{cat}$  and  $\bar{\beta}_s^\circ$  ( $r = 0.41$ ). It is important that the flexibility-mediated enhancement of the enzyme function can be brought about by mutations in the loop regions far from the

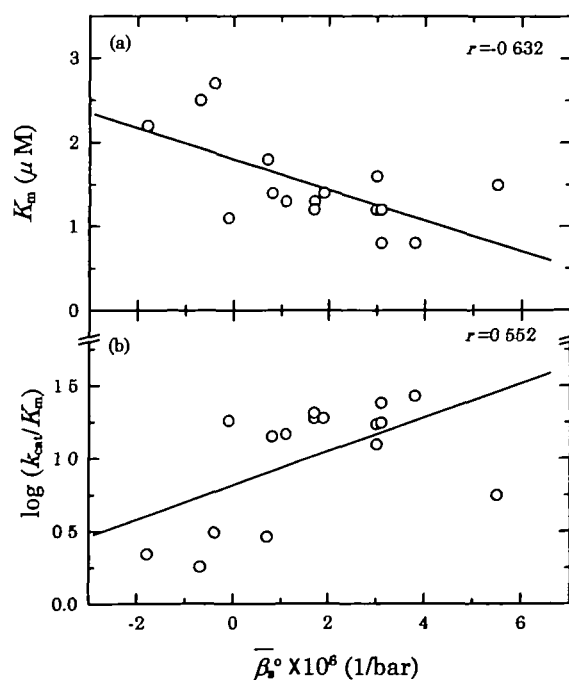


Fig. 5. Plots of  $K_m$  and  $\log(k_{cat}/K_m)$  against  $\bar{\beta}_s^\circ$  of DHFRs. Solid lines were drawn by the least-squares linear regression method.

catalytic site, because this provides a new standpoint for the molecular design of functional proteins.

There is some other experimental evidence that mutations of DHFR at positions not directly participating in the catalytic reaction affect the enzyme function by modifying the structural flexibility (1, 35, 36). We found that the rate of hydride transfer from NADPH to DHF is influenced by mutations at position 67 (23). Cameron and Benkovic (37) also revealed that the rate of hydride transfer in G121V is reduced 200-fold compared with wild-type DHFR. More interestingly, double mutations at positions 67 and 121 show nonadditive effects on stability and function, indicating that a long-range interaction exists between these two positions separated by 27.7 Å (25). These results suggest possible dynamic motions of the flexible regions of the DHFR molecule that close over both the coenzyme and substrate binding sites (1). The movie recently constructed by Sawaya and Kraut (20) demonstrates how the loops are actively and cooperatively moving to accommodate the coenzyme and substrate. We cannot derive such microscopic features of the fluctuating enzyme from the compressibility data, but comparable changes in the compressibility and internal cavities found for the kinetic intermediates (17) and for mutants at positions 67 and 121 (K. Katayanagi *et al.*, to be published) predict that the fluctuation of the DHFR molecule is basically generated through the internal cavities, which are easily modified by mutation and ligand binding.

As revealed by the present study, the adiabatic compressibility of DHFR is sensitively influenced by single amino acid substitutions in the flexible loops, due to large modifications of the internal cavity compared with surface hydration. The  $\beta_p^\circ$  value increases with an increase in  $\bar{v}^\circ$ , but it shows a tendency to decrease with the volume of the amino acid introduced. There was no significant correlation observed between  $\beta_p^\circ$  and the overall stability of the mutants as determined in the urea denaturation experiments. However, a mutant with a large  $\beta_p^\circ$  value shows high enzyme activity, mainly due to an enhanced catalytic reaction rate ( $k_{cat}$ ) and in part due to an increased affinity for the substrate ( $K_m$ ), despite the mutations in the flexible loops being far removed from the catalytic site. These findings demonstrate that a small alteration in the local structure due to mutation is dramatically magnified in the overall protein dynamics, possibly *via* "stepwise atomic reconstruction or long-range cooperative effect," and that the flexible loops of the protein play important roles in determining the enzyme function. Further insight into the molecular mechanism of mutation-induced compressibility changes will be obtained by the X-ray and high-pressure NMR analyses of these DHFR mutants now in progress.

#### REFERENCES

- Farnum, M.F., Magde, D., Howell, E.E., Hirai, J.T., Warren, M.S., Grimsley, J.K., and Kraut, J. (1991) Analysis of hydride transfer and cofactor fluorescence decay in mutants of dihydrofolate reductase: possible evidence for participation of enzyme molecular motions in catalysis. *Biochemistry* **30**, 11567–11579
- Yu, A., Ballard, L., Smilhe, L., Pearlstone, J., Foguel, D., Silva, J., Jonas, A., and Jonas, J. (1999) Effects of high pressure and temperature on the wild-type and F29W mutant forms of the N-domain of avian troponin C. *Biochim. Biophys. Acta* **1431**, 53–63
- Consonni, R., Santomo, L., Fusi, P., Tortora, P., and Zetta, L. (1999) A single-point mutation in the extreme heat- and pressure-resistant *ss07d* *Sulfolobus solfataricus* leads to a major rearrangement of the hydrophobic core. *Biochemistry* **38**, 12709–12717
- Karplus, M. and McCammon, J.A. (1981) The internal dynamics of globular proteins. *CRC Crit. Rev. Biochem.* **9**, 293–349
- Wüthrich, K. (1990) Structure and dynamics in proteins of pharmacological interest. *Biochem. Pharmacol.* **40**, 55–62
- Creighton, T.E. (1993) *Proteins—Structures and Molecular Properties*, W.H. Freeman and Company, New York
- Li, H., Yamada, H., and Akasaka, K. (1999) Effect of pressure on the tertiary structure and dynamics of folded basic pancreatic trypsin inhibitor. *Biophys. J.* **77**, 2801–2812
- Cooper, A. (1976) Thermodynamic fluctuations in protein molecules. *Proc. Natl. Acad. Sci. USA* **73**, 2740–2741
- Gekko, K. and Noguchi, H. (1979) Compressibility of globular proteins in water at 25°C. *J. Phys. Chem.* **83**, 2706–2714
- Gekko, K. and Hasegawa, Y. (1986) Compressibility-structure relationship of globular proteins. *Biochemistry* **25**, 6563–6571
- Chalikyan, T.V., Totrov, M., Abagyan, R., and Breslauer, K.J. (1996) The hydration of globular proteins as derived from volume and compressibility measurements. cross correlating thermodynamic and structural data. *J. Mol. Biol.* **260**, 588–603
- Tamura, Y. and Gekko, K. (1995) Compactness of thermally and chemically denatured ribonuclease A as revealed by volume and compressibility. *Biochemistry* **34**, 1878–1884
- Chalikyan, T.V., Gindikin, V.S., and Breslauer, K.J. (1995) Volumetric characterizations of the native, molten globule and unfolded states of cytochrome c at acidic pH. *J. Mol. Biol.* **250**, 291–306
- Kharakoz, D.P. (1997) Partial volumes and compressibilities of extended polypeptide chains in aqueous solution: additivity scheme and implication of protein unfolding at normal and high pressure. *Biochemistry* **36**, 10276–10285
- Nikitin, S.Ia., Sarvazian, A.P., and Kravchenko, N.A. (1984) Ultrasound velocimetry of lysozyme solutions. *Mol. Biol. (Mosk)* **18**, 831–838
- Gekko, K. and Yamagami, K. (1998) Compressibility and volume changes of lysozyme due to inhibitor binding. *Chem. Lett.* **839–840**
- Kamiyama, T. and Gekko, K. (2000) Effect of ligand binding on the flexibility of dihydrofolate reductase as revealed by compressibility. *Biochim. Biophys. Acta* **1478**, 257–266
- Gekko, K., Tamura, Y., Ohmae, E., Hayashi, H., Kagamiyama, H., and Ueno, H. (1996) A large compressibility change of protein induced by a single amino acid substitution. *Protein Sci.* **5**, 542–545
- Bystroff, C. and Kraut, J. (1991) Crystal structure of unliganded *Escherichia coli* dihydrofolate reductase. Ligand-induced conformational changes and cooperativity in binding. *Biochemistry* **30**, 2227–2239
- Sawaya, M.R. and Kraut, J. (1997) Loop and subdomain movements in the mechanism of *Escherichia coli* dihydrofolate reductase: crystallographic evidence. *Biochemistry* **36**, 586–603
- Gekko, K., Yamagami, K., Kunori, Y., Ichihara, S., Kodama, M., and Iwakura, M. (1993) Effects of point mutation in a flexible loop on the stability and enzymatic function of *Escherichia coli* dihydrofolate reductase. *J. Biochem.* **113**, 74–80
- Gekko, K., Kunori, Y., Takeuchi, H., Ichihara, S., and Kodama, M. (1994) Point mutations at glycine-121 of *Escherichia coli* dihydrofolate reductase: important roles of a flexible loop in the stability and function. *J. Biochem.* **116**, 34–41
- Ohmae, E., Iriyama, K., Ichihara, S., and Gekko, K. (1996) Effects of point mutations at the flexible loop glycine-67 of *Escherichia coli* dihydrofolate reductase on its stability and function. *J. Biochem.* **119**, 703–710
- Ohmae, E., Ishimura, K., Iwakura, M., and Gekko, K. (1998) Effects of point mutations at the flexible loop alanine-145 of *Escherichia coli* dihydrofolate reductase on its stability and function. *J. Biochem.* **123**, 839–846
- Ohmae, E., Iriyama, K., Ichihara, S., and Gekko, K. (1998)

- Nonadditive effects of double mutations at the flexible loops, glycine-67 and glycine-121, of *Escherichia coli* dihydrofolate reductase on its stability and function. *J Biochem.* **123**, 33–41
26. Iwakura, M. and Tanaka, T. (1992) Dihydrofolate reductase from *Bacillus subtilis* and its artificial derivatives expression, purification, and characterization. *J Biochem.* **111**, 638–642
  27. Iwakura, M., Jones, B.E., Luo, J., and Matthews, C.R. (1995) A strategy for testing the suitability of cysteine replacements in dihydrofolate reductase from *Escherichia coli*. *J Biochem.* **117**, 480–488
  28. Fierke, C.A., Johnson, K.A., and Benkovic, S.J. (1987) Construction and evaluation of the kinetic scheme associated with dihydrofolate reductase from *Escherichia coli*. *Biochemistry* **26**, 4085–4092
  29. Kauzmann, W. (1959) Some factors in the interpretation of protein denaturation. *Adv. Protein Chem.* **14**, 1–63
  30. Gekko, K. and Yamagami, K. (1991) Flexibility of food proteins as revealed by compressibility. *J Agric. Food. Chem.* **39**, 57–62
  31. Pakula, A.A. and Sauer, R.T. (1990) Reverse hydrophobic effects relieved by amino-acid substitutions at a protein surface. *Nature* **344**, 363–364
  32. Bowler, B.E., May, K., Zaragoza, T., York, P., Dong, A., and Caughey, W.S. (1993) Destabilizing effects of replacing a surface lysine of cytochrome *c* with aromatic amino acids: implications for the denatured state. *Biochemistry* **32**, 183–190
  33. Schellman, J.A. (1978) Solvent denaturation. *Biopolymers* **17**, 1305–1322
  34. Shortle, D. (1995) Staphylococcal nuclease: a showcase of m-value effects. *Adv. Protein Chem.* **46**, 217–247
  35. Ahrweiler, P.M. and Frieden, C. (1991) Effects of point mutations in a hinge region on the stability, folding, and enzymatic activity of *Escherichia coli* dihydrofolate reductase. *Biochemistry* **30**, 7801–7809
  36. Lu, L., Falzone, C.J., Wright, P.E., and Benkovic, S.J. (1992) Functional role of a mobile loop of *Escherichia coli* dihydrofolate reductase in transition-state stabilization. *Biochemistry* **31**, 7826–7833
  37. Cameron, C.E. and Benkovic, S.J. (1997) Evidence for a functional role of the dynamics of glycine-121 of *Escherichia coli* dihydrofolate reductase obtained from kinetic analysis of a site-directed mutant. *Biochemistry* **36**, 15792–15800
  38. Kraulis, P.J. (1991) MOLSCRIPT: a program to produce both detailed and schematic plots of protein structures. *J Appl. Crystallogr.* **24**, 946–950
  39. Zamyatnin, A.A. (1984) Amino acid, peptide, and protein volume in solution. *Annu. Rev. Biophys. Bioeng.* **13**, 145–165